NASA TECHNICAL MEMORANDUM

NASA TM-73792

NASA TM-73792

(NASA-TM-73792) ADHESIVE/COHESIVE STRENGTH OF A ZrO2.1-2 w/O Y2O3/NiCrAlY THERMAL BARRIER COATING (NASA) 26 p HC A03/MF A01 CSCL 11D

N78-17152

Unclas

G3/24 04467

ADHESIVE/COHESIVE STRENGTH OF A $ZrO_2 \cdot 12$ w/o Y_2O_3/NiCrAlY THERMAL BARRIER COATING

by Stanley R. Levine
Propulsion Laboratory
U.S. Army R&T Laboratories
NASA Lewis Research Center
Cleveland, Ohio 44135

TECHNICAL PAPER to be presented at the
Eightieth Annual Meeting of the American Ceramic Society
Detroit, Michigan, May 6-11, 1978

ADHESIVE/COHESIVE STRENGTH OF A

$ZrO_2 \cdot$ 12 w/o Y_2O_3/NiCrAlY THERMAL BARRIER COATING

by Stanley R. Levine

Propulsion Laboratory
U.S. Army R&T Laboratories (AVRADCOM)

E-9359

ABSTRACT

The room temperature adhesive/cohesive strength of a 0.05 cm thick $ZrO_2 \cdot$ 12 w/o Y_2O_3/0.013 cm thick NiCrAlY thermal barrier coating system (TBC) was investigated. The weakest link was the oxide/NiCrAlY interface region with a strength of 6.2 MN/m^2. The fracture was about half cohesive oxide failure, half oxide/NiCrAlY adhesive failure and 1 percent cohesive NiCrAlY failure. The TBC failed in a similar manner in 950° C tensile and compression tests. The oxide stripped from the TBC had a cohesive strength of 24.6 MN/m^2. The NiCrAlY had a cohesive strength of 25.1 MN/m^2. The NiCrAlY and oxide failed primarily at interparticle boundaries.

E-9359

ADHESIVE/COHESIVE STRENGTH OF A

$ZrO_2 \cdot$ 12 w/o Y_2O_3/NiCrAlY THERMAL BARRIER COATING

by Stanley R. Levine

Propulsion Laboratory
U.S. Army R&T Laboratories (AVRADCOM)

SUMMARY

A study of the room temperature adhesive/cohesive strength of a 0.05 cm thick $ZrO_2 \cdot$ 12 w/o Y_2O_3/0.013 cm thick NiCrAlY thermal barrier coating system (TBC) and its component layers was carried out. The as-deposited coatings were characterized to serve as a reference condition for EDAX, SEM and metallographic studies of the adhesive/cohesive strength specimens. Mechanically induced 950° C tensile and compressive coating failures were examined to assess the propriety of the adhesive/cohesive strength test.

The weakest link in the thermal barrier coating was the oxide/NiCrAlY interface region with a room temperature strength of 6.2 MN/m^2. The fracture mode was about half cohesive oxide failure, half oxide/NiCrAlY adhesive failure and 1 percent cohesive NiCrAlY failure. The TBC also failed in 900 to 950° C tensile and compression tests in the oxide/NiCrAlY interface region. As in the adhesive/cohesive strength test, the fracture path ran through the first deposited oxide as well as along the oxide NiCrAlY interface. The oxide stripped from the TBC had a cohesive strength of 24.6 MN/m^2. In all cases the oxide fracture path ran primarily along interparticle boundaries.

The 0.050 cm thick NiCrAlY coating had a cohesive strength of 25.1 MN/m^2. The 0.013 cm thick NiCrAlY coating/epoxy joint had a strength of 37.6 MN/m^2 (epoxy adhesive/cohesive strength = 50.3 MN/m^2). The fracture path for NiCrAlY primarily ran along interparticle boundaries.

STAR Category 26

Based on the results of this study the adhesive/cohesive strength test appears to be a useful diagnostic, coating development and quality control tool.

INTRODUCTION

The addition of an insulating coating to the outer airfoil surfaces of cooled turbine blades or vanes is an atttractive approach to extending the turbine inlet temperature capability of gas turbines with current generation alloys. This approach to the use of thermal barrier coatings (TBC) can give large benefits in cycle efficiency. The potential benefits may also be taken more directly through metal temperature reduction and longer life (1).

A plasma spray deposited TBC system comprised of a 0.02 to 0.07 cm 12 w/o Y_2O_3 stabilized ZrO_2 outer insulating layer and a 0.008 to 0.018 cm Ni-16 Cr-5.6Al-0.6Y inner bond coat has been identified at NASA Lewis (2, 3). In cyclic furnace endurance tests this system was superior to similar coatings having CaO or MgO stabilized ZrO_2 as the insulating layer (2). All three coatings successfully survived 500 cycles between full power and flame out on the first stage blades of a J-75 test stand engine. The success of this test generated a greal deal of interest in thermal barrier coatings throughout the gas turbine industry (1, 4).

Among the key steps in the commercialization of any new material are mechanical property characterization and the development of quality assurance procedures. This study of the bond strength of the ZrO_2-12 w/o Y_2O_3/NiCrAlY TBC system addresses both of these questions. The primary purpose of this study was to quantitatively determine the adhesive or cohesive strength of the thermal barrier coating and its component layers in the as-deposited condition at room temperature. An additional purpose was to characterize each fracture as to the extent to which it was adhesive or cohesive and intergranular to transgranular by metallography, scanning electron microscopy (SEM), and energy dispersive analysis of X-rays (EDAX). Finally, the nature of the coating fracture in this test was compared to mechanically induced 900 to 950° C tensile and compressive coating failures to assess the relevance of the room temperature adhesive/cohesive strength test.

EXPERIMENTAL PROCEDURES

The coatings subjected to adhesive/cohesive strength testing (5) were 0.013 cm thick and 0.05 cm thick plasma sprayed NiCrAlYs and the plasma sprayed TBC system (0.050 cm thick ZrO_2-12 w/o Y_2O_3 insulating layer on a 0.013 cm thick NiCrAlY bond coat). The coatings were applied to the degreased and grit blasted face of IN-718 coating fixtures as illustrated in figure 1. The nominal ZrO_2-12 w/o Y_2O_3 contained 11.8 w/o Y_2O_3 and minor element concentrations differing slightly from the 12 w/o Y_2O_3 material used by Stecura (2). The NiCrAlY powder and coating application procedures, plasma spray equipment and equipment operator were the same as used by Stecura. The coated fixtures were placed in assembly dies and coated with 0.005 to 0.010 cm of aluminum filled epoxy. The degreased and grit blasted loading fixture and 2.25 kg compressive load were applied and the assemblies, figure 1, were cured for one hour at 150° C. After curing the assembly dies were removed. Excess epoxy was removed from the periphery of the joints. The assemblies were then tensile tested and loads to fracture recorded. Epoxy joints alone were also tested.

Since the thermal barrier coatings failed close to the oxide/bond coat interface, the bulk of the oxide layer and the epoxy transferred to the loading fixture essentially in tact. New loading fixtures were epoxied to the transferred oxides so that the bulk oxide could also be tested. All tests were run at least in duplicate.

The failed joints were photographed at ×2 magnification. One set of coating and loading fixtures for each joint type tested was sectioned through the assembly center line and examined metallographically. Another set was prepared for SEM and EDAX examination by vacuum depositing a small quantity of gold on the fracture surfaces. SEM and EDAX were done on a JEOL SEM at 25 kV, 15^o tilt. EDAX was carried out in the integral mode with 50 ev/channel, a counting time of 100 seconds, and the magnification at ×60. The as-deposited TBC was also characterized by metallography, SEM and EDAX to serve as a reference condition.

RESULTS AND DISCUSSION

As-Deposited Coating Structure

A photomicrograph of the thermal barrier coating system deposited on IN-718 is shown in figure 2. The oxide and metallic layers have laminated structures typical of plasma sprayed deposits. The NiCrAlY layer has some porosity and oxide inclusions. The large inclusions at the NiCrAlY/IN-718 interface are Al_2O_3 grit blasting particles. NiCrAlY particle boundaries are frequently delineated by oxide films. The ZrO_2 layer has about 10 percent porosity. Some of the larger pores are due to pullout during metallographic preparation. SEM examination revealed a surface structure similar to parafin candle drippings for both layers (figs. 2(b) and (c)). The oxide had a network of coarse and fine cracks as can be seen from the sequence of photos in figures 2(c) to (e).

Adhesive/Cohesive Strength and Failure Mode

Adhesive/cohesive strength data and qualitative comments about the type of failure and failure location for each specimen are summarized in table I. Photomacrographs of each failed joint type are shown in figure 3.

Epoxy. - The epoxy, figure 3(a), had an average adhesive/cohesive strength of 50.3 MN/m^2.

NiCrAlY (0.013 cm thick). - This joint, figure 3(b), failed at an average stress of 37.6 MN/m^2. The failure was probably of the mixed cohesive/adhesive type with the fracture path running through both the

NiCrAlY and the epoxy and along the interface between them. Thus, these results do not have the sought after direct meaning in terms of the strength of the NiCrAlY layer of the TBC system. The failure mode is illustrated in figure 4. The upper and lower halves of this and succeeding similar metallographic pairs do not mate along the fracture path. Figure 4(a) reveals that the joint failed partially by decohesion of the NiCrAlY along interparticle boundaries as can be seen at the left, lower half. The light plate-like material on the upper half is NiCrAlY transferred to the epoxy. The SEM of surface A, figure 4(b), reveals that the epoxy (dark areas) also failed cohesively and transferred to the NiCrAlY in some areas.

NiCrAlY (0.050 cm thick). - The fracture of this coating, figure 3(c), was essentially entirely cohesive. The average cohesive strength of the NiCrAlY was 25.1 MN/m^2. As can be seen from figure 5(a) the NiCrAlY failed primarily at interparticle boundaries along a path close to the NiCrAlY/IN-718 fixture interface. The SEM of surface A, figure 5(b), clearly reveals the integranular nature of the fracture. Areas on this fracture surface are similar to certain areas of the as-deposited NiCrAlY surface (fig. 2(b)). The strength of the 0.013 NiCrAlY/epoxy joint discussed above falls between the measured adhesive/cohesive strength of the epoxy and the measured cohesive strength of the 0.050 cm thick NiCrAlY.

Thermal Barrier Coating. - The 0.05 cm $ZrO_2 \cdot$ 12 w/o Y_2O_3/0.013 cm NiCrAlY TBC system failed in the oxide/bond coat interface region (fig. 3(d)). The average failure stress was 6.2 MN/m^2. As can be seen from figures 6(a) and (b) the fracture path ran through both the oxide and along the oxide/NiCrAlY interface. This region is the weakest link of the TBC. The oxide is the light, fine structured material on surface A in figure 6(b). Very little NiCrAlY adhered to the stripped oxide (upper part of fig. 6(a)). Thus the fracture is of the mixed cohesive/adhesive type. Figures 6(c) and (d) reveal that the oxide fractured primarily in an interparticle mode. The dark smooth area at the lower left of these figures is NiCrAlY. Figure 6(e) is an SEM of surface B of the stripped off oxide. The crack networks and solidified droplet character of surfaces A and B are similar to the features found on the surface of the as-sprayed oxide (figs. 2(c) to (e)).

$ZrO_2 \cdot 12$ w/o Y_2O_3. - The stripped 0.05 cm oxide from the TBC system failed cohesively as can be seen from figures 3(e) and 7(a). The average cohesive strength was 24.6 MN/m^2. The fracture followed a primarily intergranular path (figs. 7(b) and (c)).

Quantitative Determination of the Fracture Mode of the TBC

The EDAX feature of the SEM was used to quantitatively characterize the fracture surfaces of the TBC. The EDAX data are summarized in table II. The oxide and NiCrAlY cohesive failure specimens were used to establish the TBC fracture area calibration graph shown in figure 8(a). Surface A, figure 6(a) (adhering NiCrAlY plus oxide), had 45 to 53 percent oxide coverage based on an average analysis from 17 EDAX measurements. The stripped oxide plus adhering NiCrAlY (surface B, fig. 6(a)) had only 1 percent NiCrAlY coverage. Therefore the fracture path was approximately 50 percent oxide cohesive failure, 50 percent oxide/NiCrAlY adhesive failure with about 1 percent NiCrAlY cohesive failure. Joint strength is plotted against failure mode in figure 8(b) for the TBC. These data indicate that the adhesive strength is either very low and/or that the first deposited oxide layers are substantially weaker than successive layers.

Elevated Temperature Failure Mode

The propriety of the room temperature adhesive/cohesive strength tests carried out in this study is supported by the results of 900 to 950° C tensile and compression tests of thermal barrier coated IN-100. As can be seen from the photomacrographs in figure 9(a) the coatings failed in the vicinity of the oxide/NiCrAlY interface. Metallographic examination of a longitudinal section of the tensile specimen (fig. 9(b)) reveals a fracture path similar to the path in the adhesive/cohesive strength tests of the TBC, that is, through the first deposited oxide layers as well as along the oxide/NiCrAlY interface. In the compression test, figure 9(c), the fracture path tended to run more in the oxide. In both tests the oxide failed primarily in an interparticle mode. Evidence of NiCrAlY failure along interparticle boundaries is evident in the microstructure of the tensile test specimen.

Failures of the TBC in the vicinity of the oxide/NiCrAlY interface have also been observed in unreported stress-rupture tests on thermal barrier coated gas turbine alloys conducted by the author.

CONCLUDING REMARKS

In both the elevated temperature tests and the room temperature adhesive/cohesive strength tests, the weakest link in the thermal barrier coatings was revealed to be the oxide/NiCrAlY adhesive bond and the cohesive strength of the first deposited oxide layers. Based on these observations it appears as though the room temperature adhesive/cohesive strength test is of value as a diagnostic, coating development and quality control tool.

The low adhesive strength at the oxide/NiCrAlY interface and the low cohesive strength of the first deposited oxide layers may be due to the deposition procedure. The first oxide layers are plasma spray deposited on a cold high thermal conductivity substrate and thus suffer greater thermal shock than successive layers which are deposited on the warm low conductivity oxide (steady state temperature of about 250° C). This suggests that deposition of the oxide on a preheated substrate may strengthen the oxide/NiCrAlY interface region of the thermal barrier coating.

SUMMARY OF RESULTS

A study of the room temperature adhesive/cohesive strength of a 0.05 cm thick $ZrO_2 \cdot 12$ w/o Y_2O_3/0.013 cm thick NiCrAlY thermal barrier coating system (TBC) and its component layers was carried out. The as-deposited layers and coating were characterized as a reference condition for EDAX, SEM, and metallographic studies of the failed adhesive/cohesive strength specimens. Mechanically induced 900 to 950° C tensile and compressive coating failures were examined to assess the propriety of the adhesive/cohesive strength test. The following results were obtained:

1. The weakest link in the TBC was the oxide/NiCrAlY interface region with a strength of 6.2 MN/m^2. The fracture mode was about half cohesive oxide failure, about half oxide/NiCrAlY adhesive failure and about 1 percent cohesive NiCrAlY failure. The oxide failed primarily at interparticle boundaries.

2. The TBC failed in both the room temperature adhesive/cohesive strength test and 900 to 950° C tensile and compression tests in the oxide/NiCrAlY interface region. In all cases the fracture path ran through the first deposited oxide layers as well as along the oxide NiCrAlY interface.

3. The oxide stripped from the TBC had a cohesive strength of 24.6 MN/m^2 with the fracture path running primarily along interparticle boundaries.

4. The 0.050 cm thick NiCrAlY coating had a cohesive strength of 25.1 MN/m^2. The fracture path ran primarily along interparticle boundaries. A more representative 0.013 cm thick NiCrAlY coating had a joint strength of 37.6 MN/m^2. However, the fracture consisted of cohesive failure of the NiCrAlY and epoxy (epoxy cohesive strength = 50.3 MN/m^2) and adhesive failure between the NiCrAlY and epoxy. Strength was intermediate between the epoxy and 0.050 NiCrAlY joint strengths. Again, the NiCrAlY failed at interparticle boundaries.

REFERENCES

1. F. S. Stepka, C. H. Liebert, and S. Stecura, "Summary of NASA Research on Thermal-Barrier Coatings," NASA TM X-73584, 1977.

2. S. Stecura, "Two-Layer Thermal Barrier Coating for Turbine Airfoils-Furnace and Burner Rig Test Results," NASA TM X-3425, Sept. 1976.

3. C. H. Liebert, et al., "Durability of Zirconia Thermal-Barrier Ceramic Coatings on Air-Cooled Turbine Blades in Cyclic Jet Engine Operation," NASA TM X-3410, Sept. 1976.

4. S. R. Levine and J. S. Clark, "Thermal Barrier Coatings - A Near Term, High Payoff Technology," NASA TM X-73586, 1977.

5. "Standard Method for Adhesion or Cohesive Strength of Flame - Sprayed Coatings," ASTM C633-69, 1969.

TABLE I. - ADHESIVE/COHESIVE STRENGTH DATA

Joint structure	Bond coat thickness, cm	Oxide thickness, cm	Bond strength, MN/m^2	Type of failure	Failure location
Epoxy	0	0	50.0	Cohesive/Adhesive	Epoxy
Epoxy	0	↓	50.6	Cohesive/Adhesive	Epoxy
NiCrAlY	.013		41.1	Cohesive/Adhesive	Epoxy/NiCrAlY
↓	.013		34.0	Cohesive/Adhesive	Epoxy/NiCrAlY
	.05		21.5	Cohesive	NiCrAlY
	.05		28.6	Cohesive	NiCrAlY
$ZrO_2 \cdot 12$ w/o Y_2O_3/NiCrAlY	.013	.05	3.7	Cohesive/Adhesive	Oxide/NiCrAlY
↓	↓	↓	7.1	↓	↓
			6.3		
			7.6		
$ZrO_2 \cdot 12$ w/o Y_2O_3	0		24.1	Cohesive	Oxide
$ZrO_2 \cdot 12$ w/o Y_2O_3	0		25.0	Cohesive	Oxide

TABLE II. - EDAX ANALYSIS OF THE TBC FRACTURE SURFACES

Joint structure	Analyzed surface	Metallic element content, wt %[a]					Fracture areas, %	
		Ni	Cr	Al	Y	Zr	NiCrAlY	$ZrO_2 \cdot Y_2O_3$
NiCrAlY (0.05 cm)	Cohesive failure of NiCrAlY	68	26	7.9	[b]----	----	100	0
$ZrO_2 \cdot$ 12 w/o Y_2O_3	Cohesive failure of oxide	----	--	---	11.5	88.5	0	100
$ZrO_2 \cdot$ 12 w/o Y_2O_3/NiCrAlY	Adhering NiCrAlY + oxide	31	12	4.8	5.2	47	47-53	47-53
$ZrO_2 \cdot$ 12 w/o Y_2O_3/NiCrAlY	Stripped oxide + adhering NiCrAlY	1.1	--	---	11	88	1	99

[a]SEM EDAX: ×60 magnification, 15° tilt, 25 kV

$$\% M_i = \frac{M_i - M_{i\,(background)}}{\sum_{i=1}^{n} \left[M_i - M_{i\,(background)} \right]} \times 100.$$

[b]Not determined.

ORIGINAL PAGE IS OF POOR QUALITY

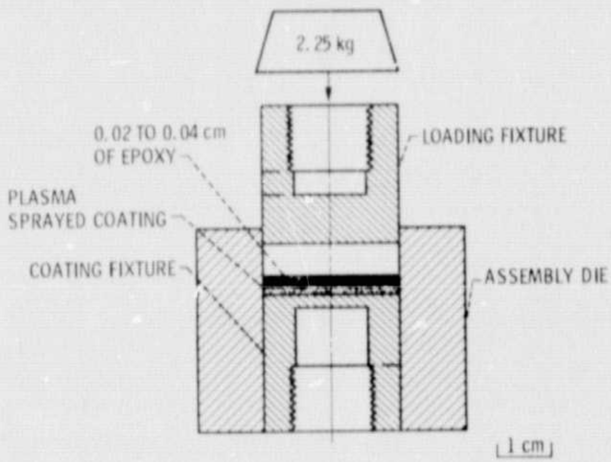

Figure 1. - Adhesive/cohesive strength specimen assembly prior to curing the epoxy. The assembly die is removed after curing.

ORIGINAL PAGE IS
OF POOR QUALITY

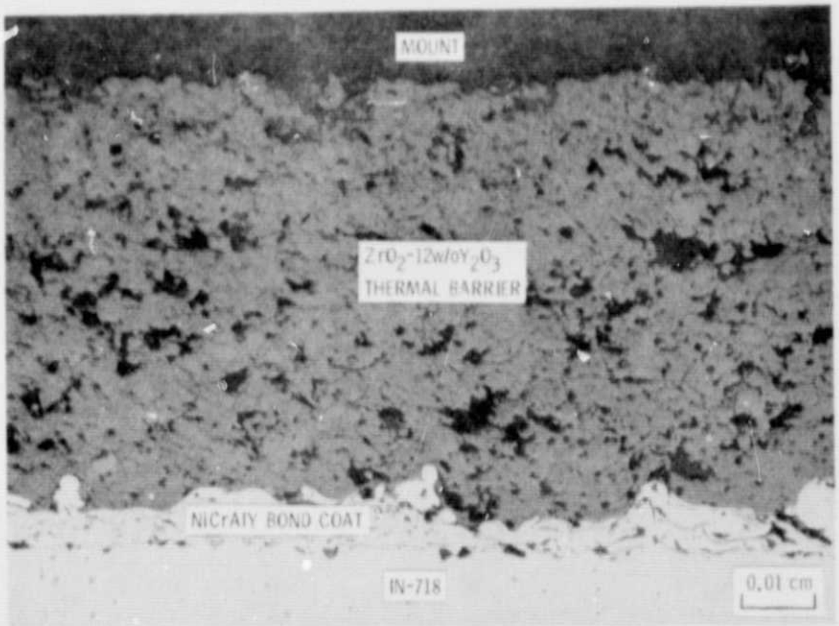

(a) MICROSTRUCTURE.

Figure 2. - As-plasma spray deposited thermal barrier coating structure.

E-1359

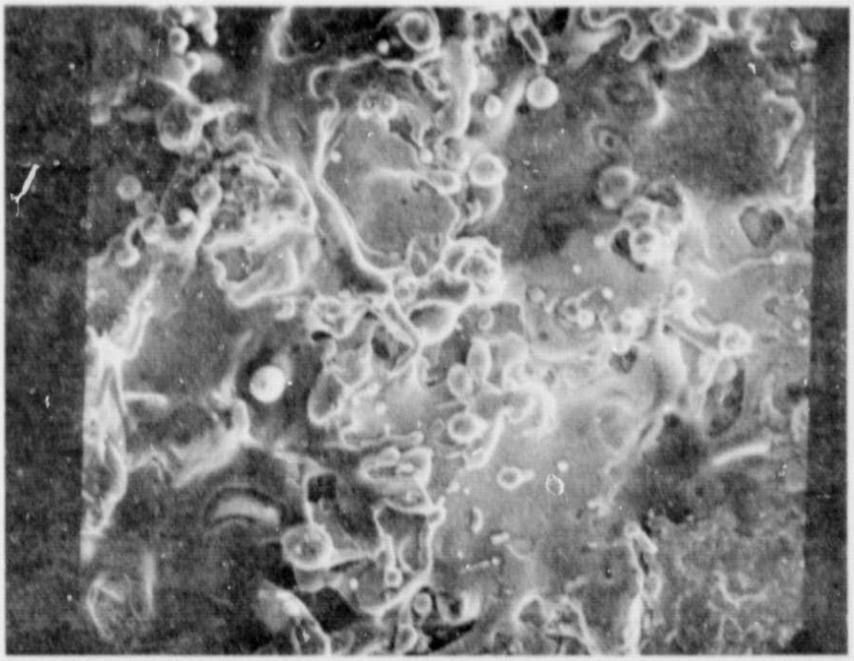

(b) SEM of as-deposited NiCrAlY surface at X300.

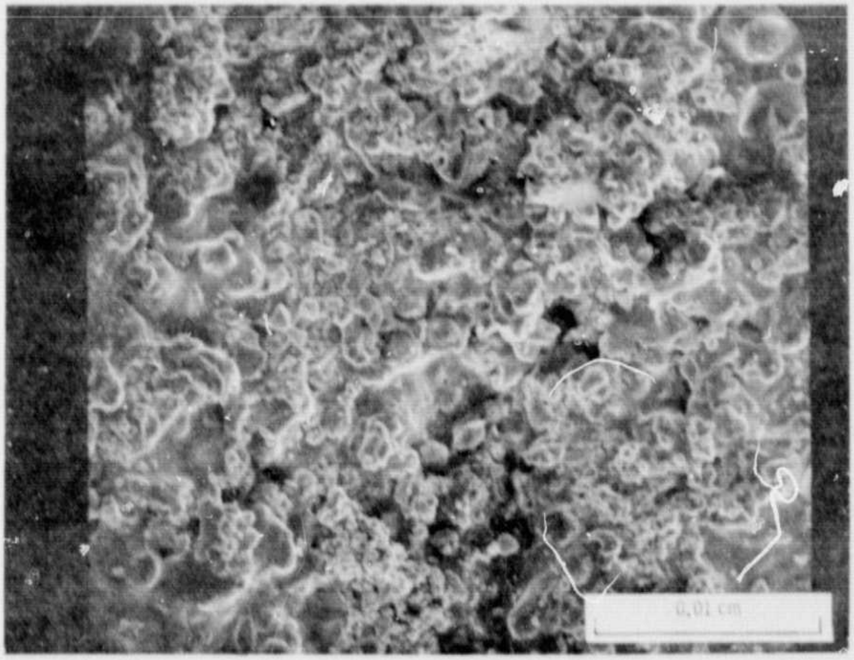

(c) SEM of as-deposited oxide surface at X300.

Figure 2. - Continued.

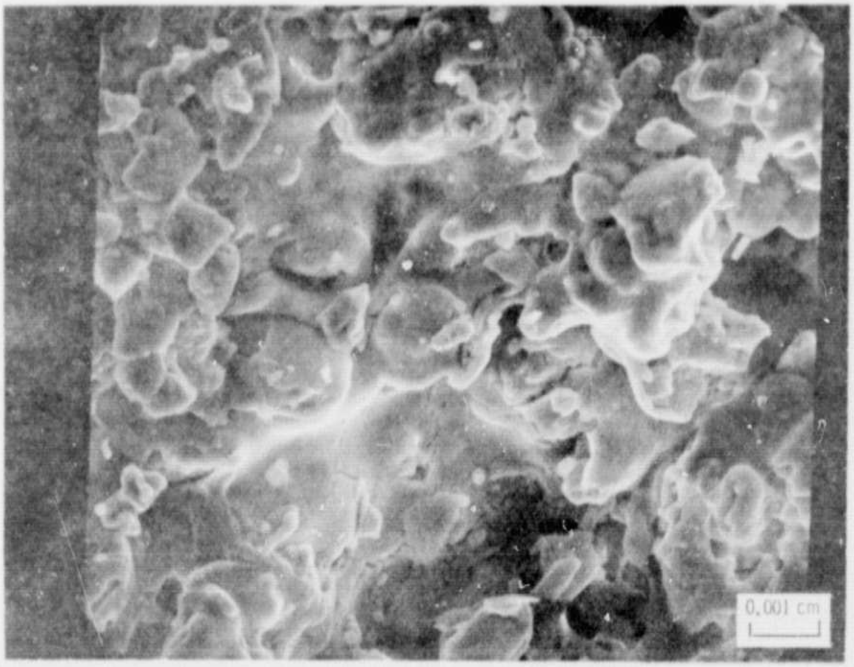

(d) SEM of as-deposited oxide surface at X1000.

E-1359

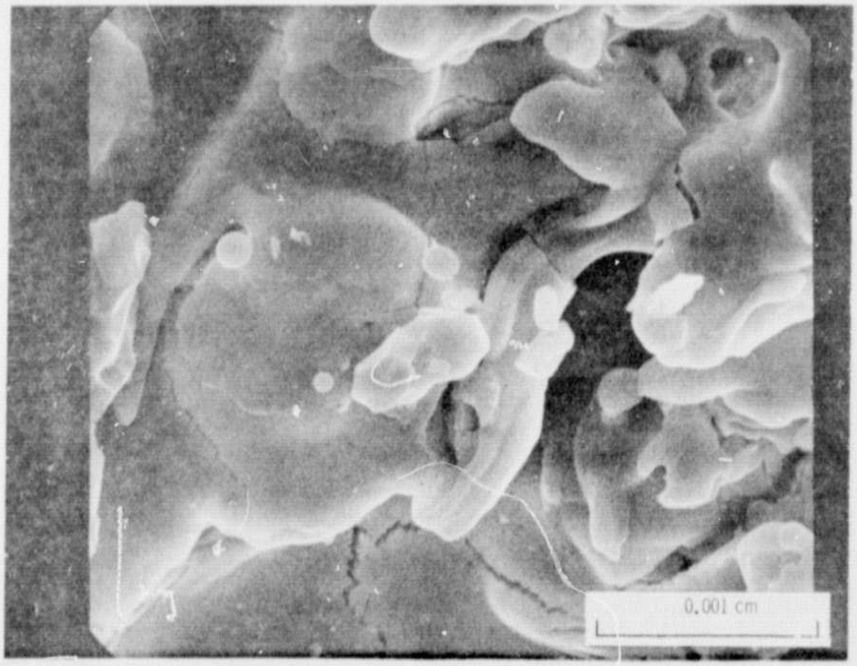

(e) SEM of as-deposited oxide surface at X3000.

Figure 2. - Concluded.

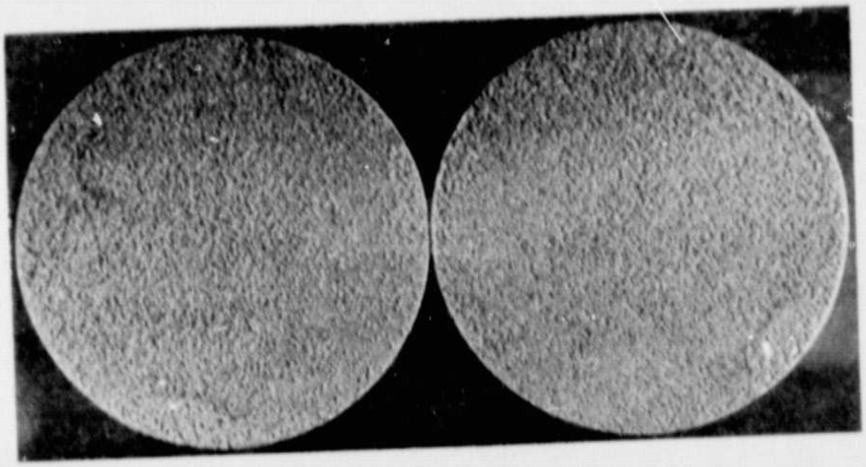

(a) EPOXY.

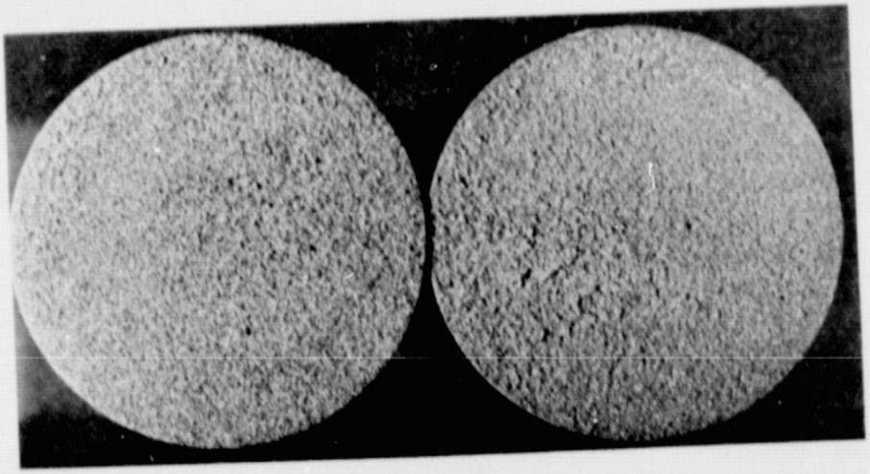

(b) 0.013 cm NiCrAlY BOND COAT.

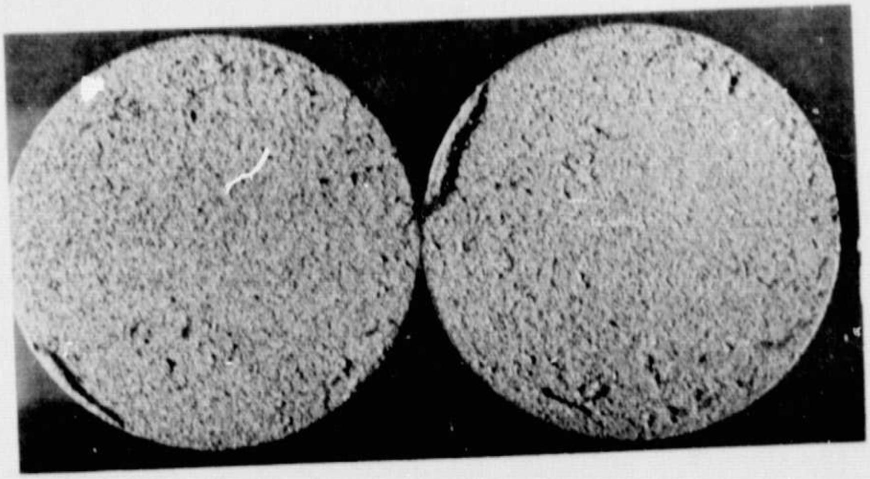

(c) 0.05 cm NiCrAlY BOND COAT.

Figure 3. - Photomacrographs of fracture surfaces. The specimens on which the plasma sprayed coatings were depositied are on the left (b, c, d).

ORIGINAL PAGE IS
OF POOR QUALITY

E-9359

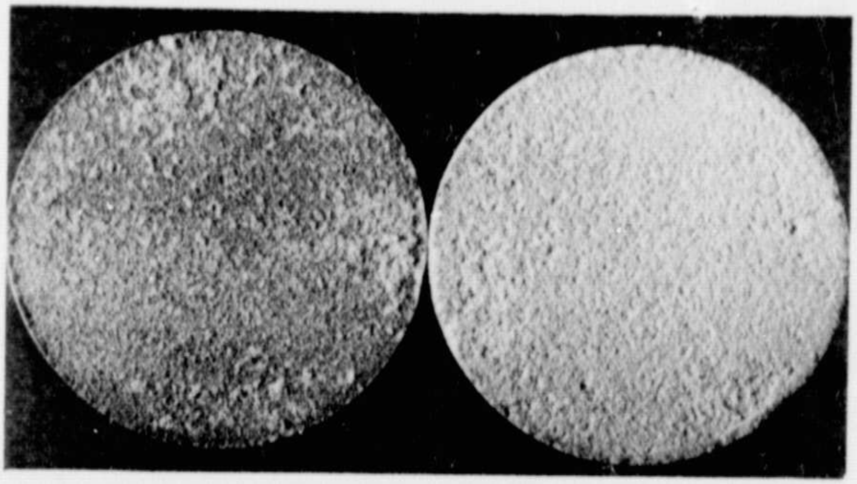

(d) THERMAL BARRIER COATING: 0.05 cm ZrO_2-12 w/o Y_2O_3, 0.013 cm NiCrAlY.

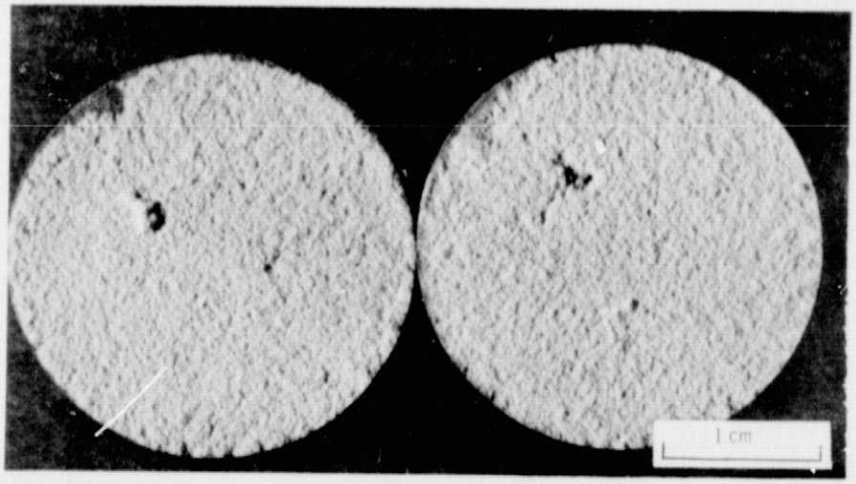

(e) 0.05 cm ZrO_2-12 w/o Y_2O_3.

Figure 3. - Concluded.

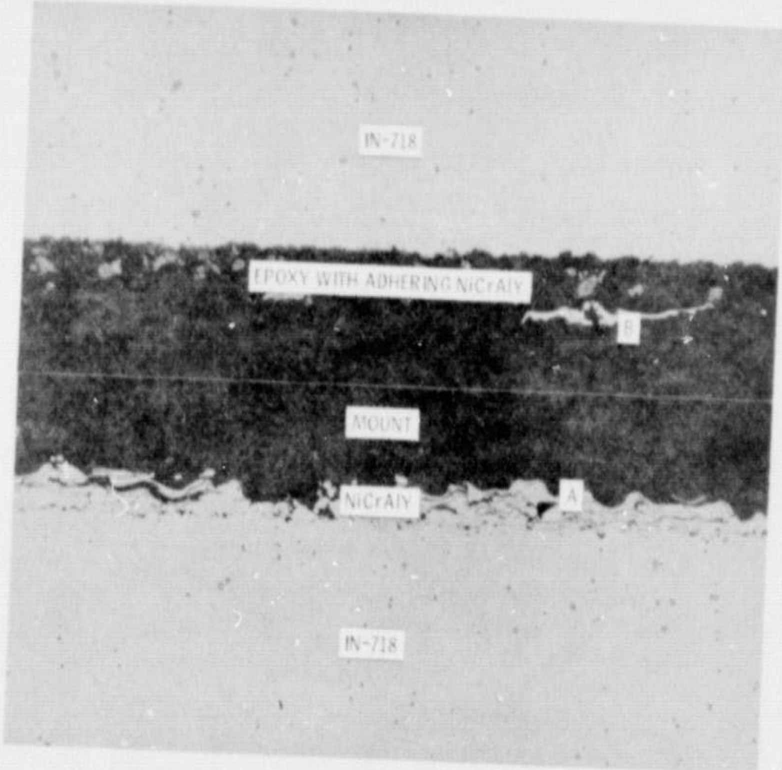

(a) MICROSTRUCTURE OF TESTED 0.013 cm NiCrAlY BOND COAT.

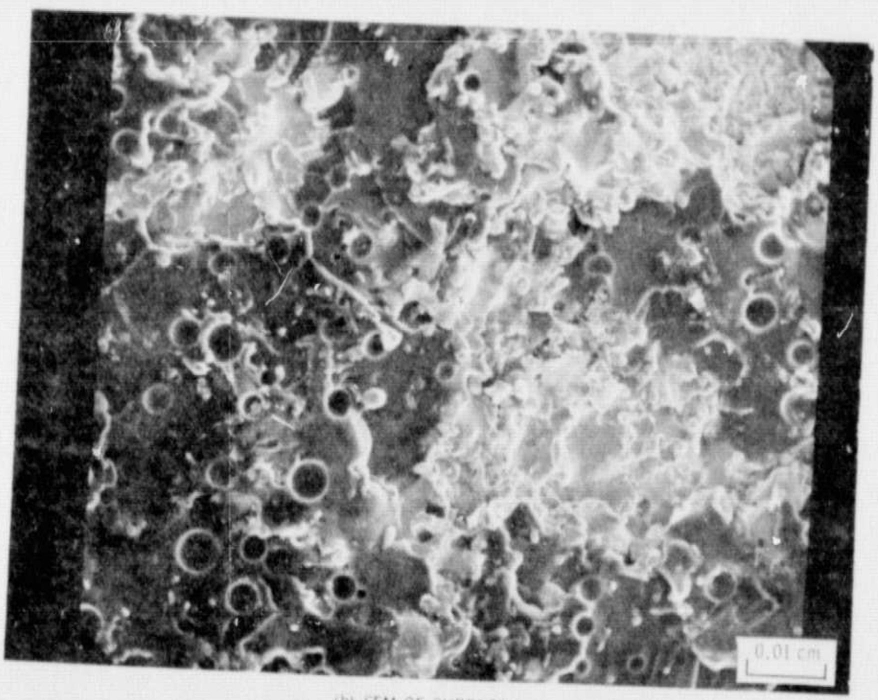

(b) SEM OF SURFACE A.

Figure 4. - Characterization of 0.013 cm NiCrAlY adhesive/adhesive coating fracture.

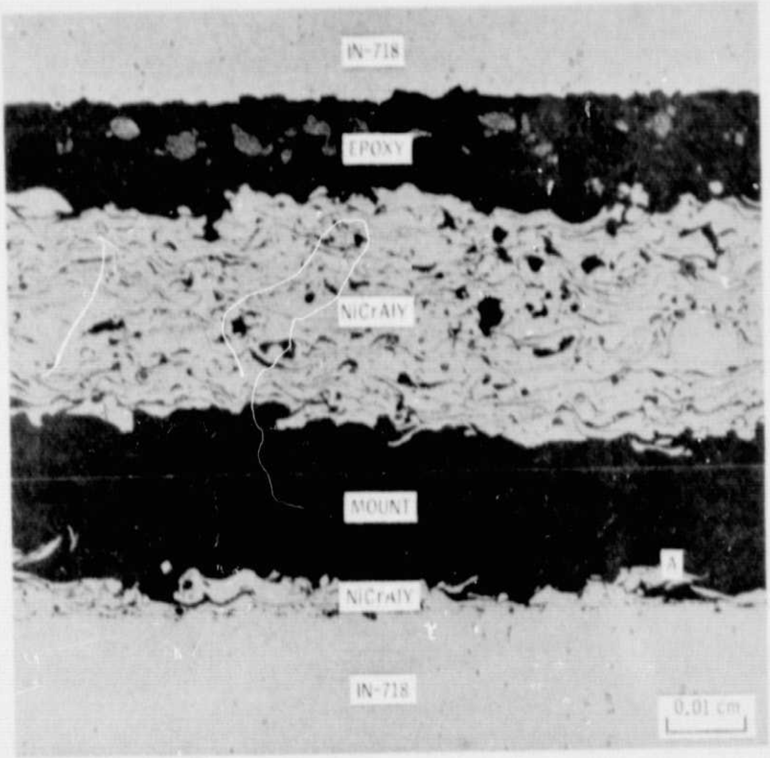

(a) MICROSTRUCTURE OF TESTED 0.05 cm NiCrAlY BOND COAT.

(b) SEM OF SURFACE A.

Figure 5. - Characterization of 0.05 cm NiCrAlY cohesive coating fracture.

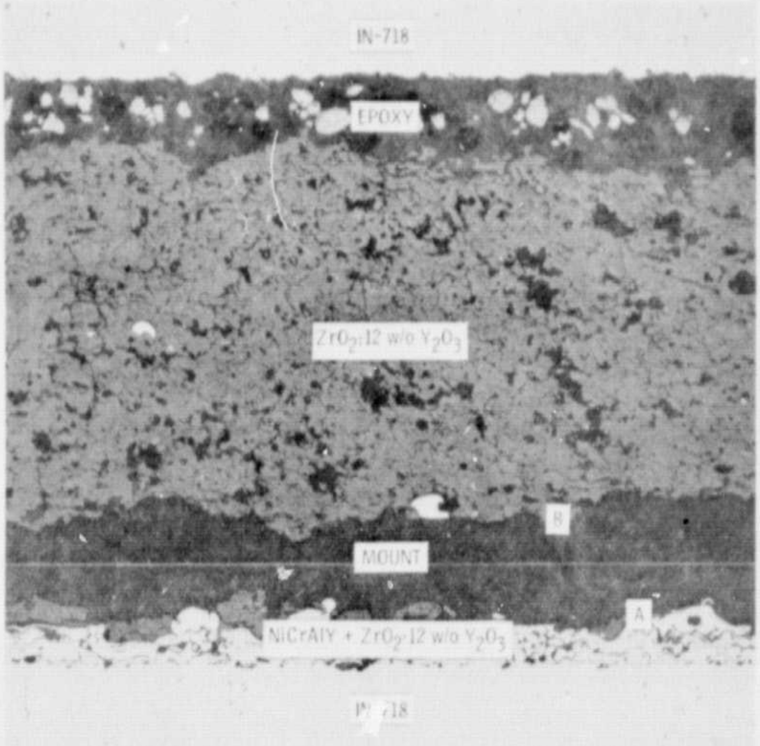

(a) MICROSTRUCTURE OF TESTED THERMAL BARRIER COATING.

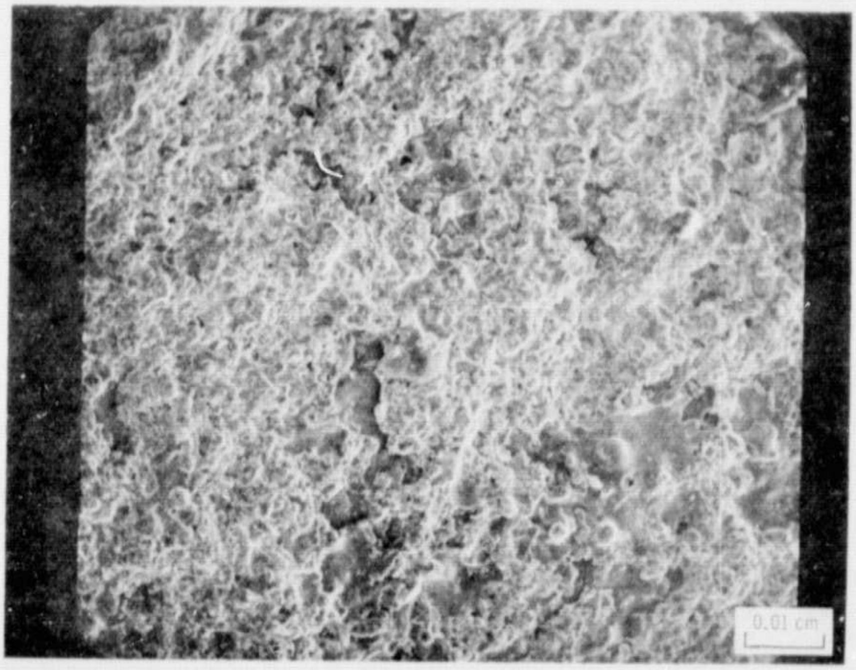

(b) SEM OF SURFACE A, X100.

Figure 6. - Characterization of thermal barrier coating cohesive/adhesive fracture.

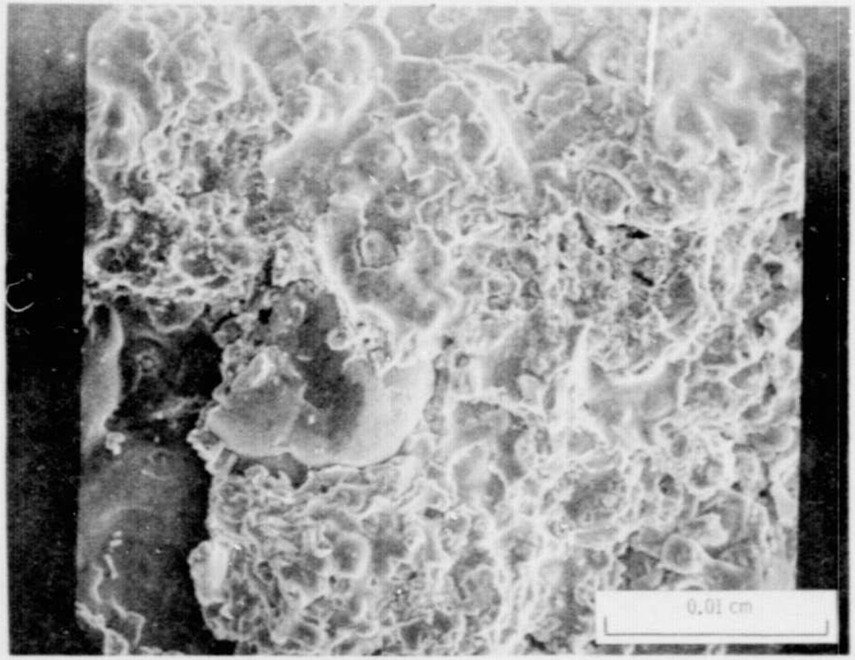

(c) SEM OF SURFACE A, X300.

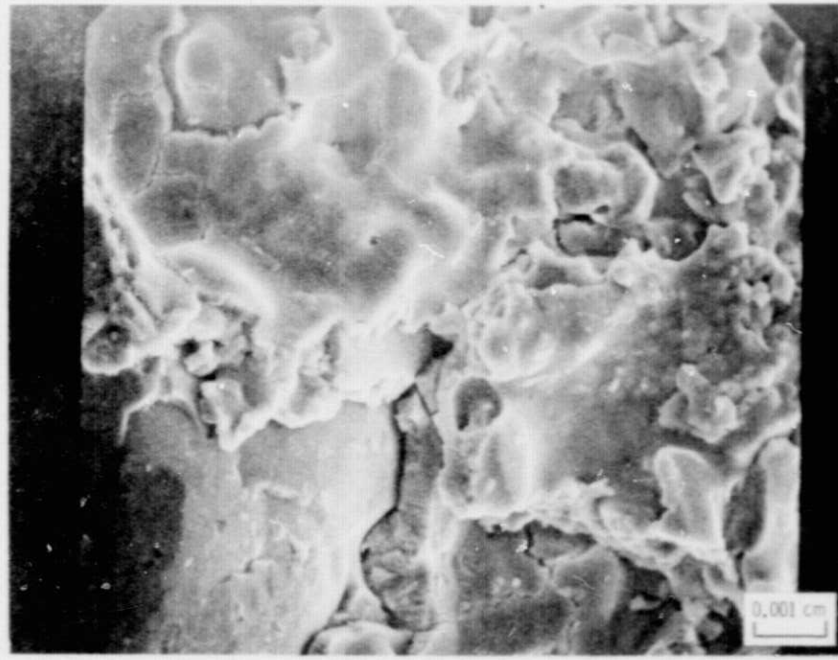

(d) SEM OF SURFACE A, X1000.

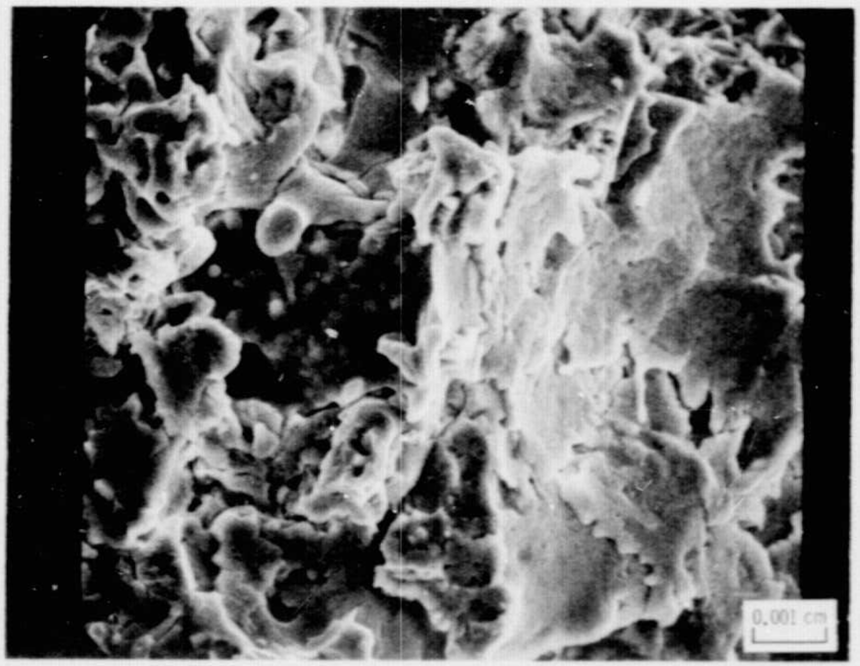

(e) SEM OF SURFACE B, X1000.

Figure 6. - Concluded.

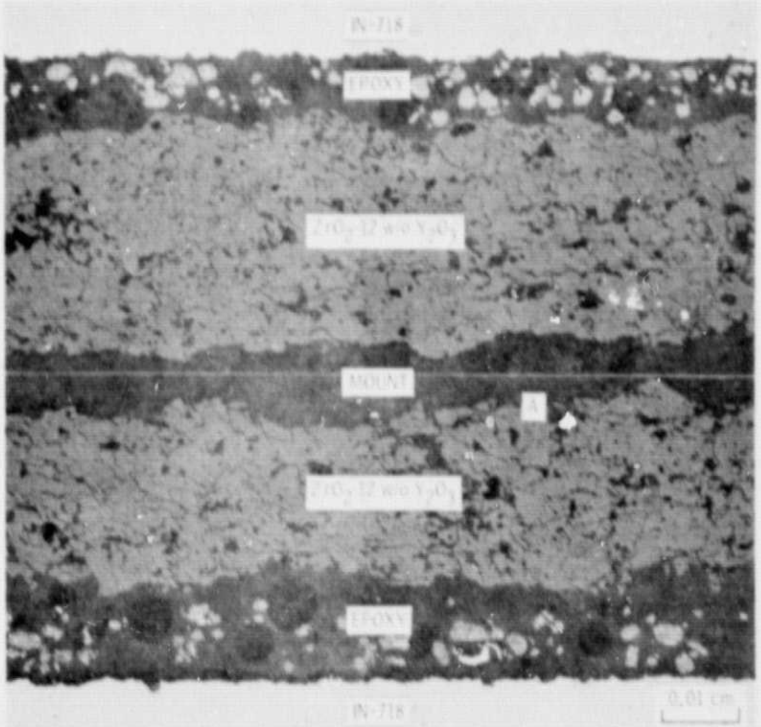

(a) MICROSTRUCTURE OF TESTED ZrO_2-12 w/o Y_2O_3.

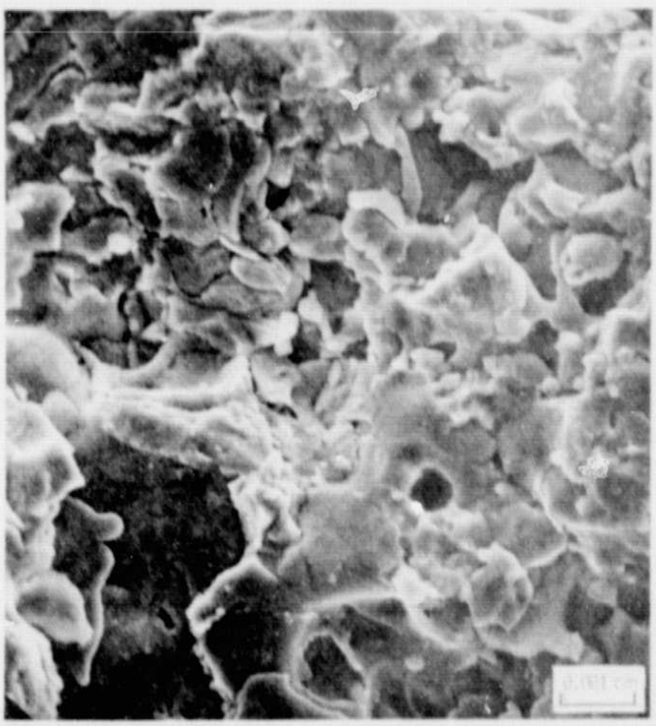

(b) SEM OF SURFACE A, X1000.

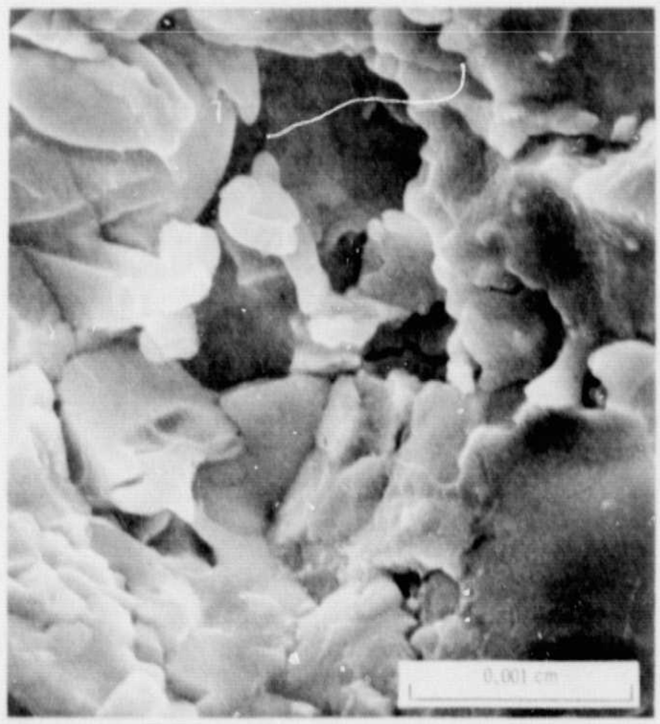

(c) SEM OF SURFACE A, X3000.

Figure 7. - Characterization of ZrO_2-12 w/o Y_2O_3 cohesive fracture.

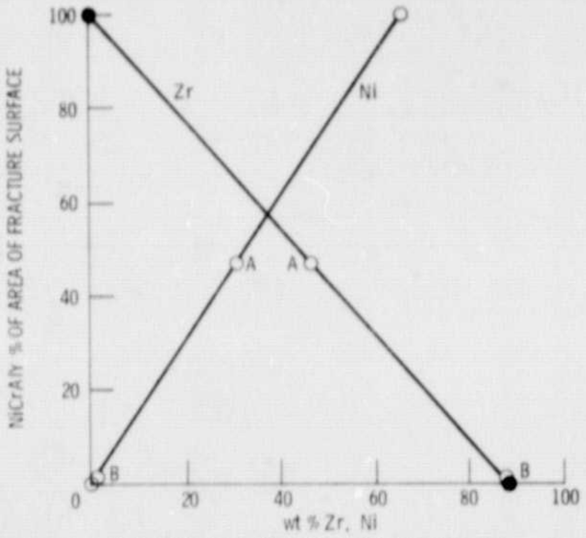

(a) FRACTURE AREA CALIBRATION GRAPH FOR $ZrO_2 \cdot 12$ w/o Y_2O_3/NiCrAlY.

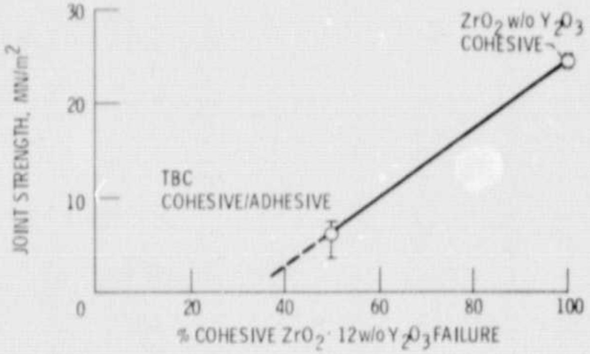

(b) CORRELATION OF JOINT STRENGTH WITH FAILURE MODE FOR THE TBC.

Figure 8. - Quantitative determination of fracture mode for the thermal barrier coating.

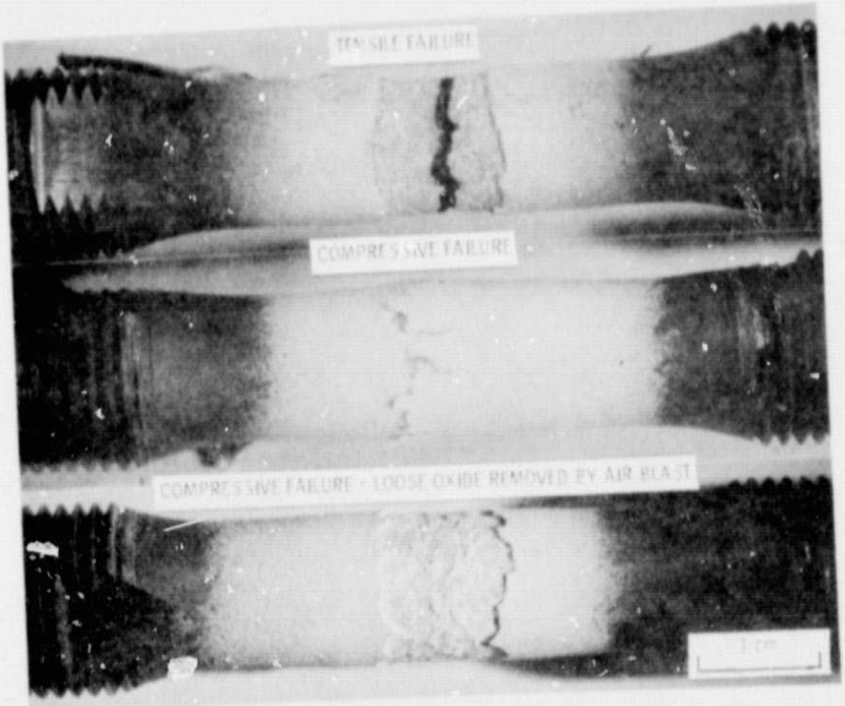

(a) PHOTOMACROGRAPHS OF MECHANICALLY INDUCED TBC FAILURES.

(b) PHOTOMICROGRAPH OF TENSILE SPECIMEN.

Figure 9. - Mechanically induced thermal barrier coating failures on IN-100 at 900 to 950° C.

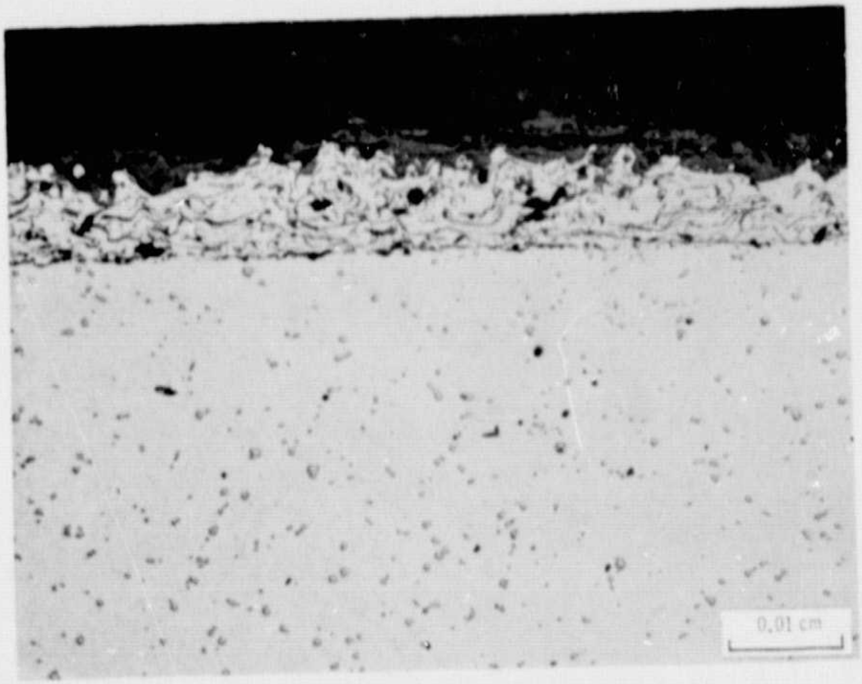

(c) PHOTOMICROGRAPH OF COMPRESSION SPECIMEN.

Figure 9. - Concluded.

NASA-Lewis-Com'l